Atmos. Chem. Phys. Discuss., https://doi.org/10.5194/acp-2018-1034
Manuscript under review for journal Atmos. Chem. Phys.
Discussion started: 6 December 2018
© Author(s) 2018. CC BY 4.0 License.

Atmospheric Chemistry and Physics Discussions

Extending the SBUV PMC Data Record with OMPS NP

Matthew T. DeLand[1] and Gary E. Thomas[2]

[1]Science Systems and Applications, Inc. (SSAI), Lanham, Maryland 20706 USA

[2]Laboratory for Atmospheric and Space Physics (LASP)/University of Colorado, Boulder, Colorado 80303 USA

Correspondence to: Matthew DeLand (matthew.deland@ssaihq.com)

Abstract. We have utilized Solar Backscatter Ultraviolet (SBUV) instrument measurements of atmospheric radiance to create a 40-year record of polar mesospheric cloud (PMC) behavior. While this series of measurements is nearing its end, we show in this paper that Ozone Mapping and Profiling Suite (OMPS) Nadir Profiler (NP) instruments can be added to the merged SBUV PMC data record. Regression analysis of this extended record shows smaller trends in PMC ice water content (IWC) since approximately 1998, consistent with previous work. Current trends are statistically significant in the Northern Hemisphere, but not in the Southern Hemisphere. The PMC IWC response to solar activity has decreased in the Northern Hemisphere since 1998, but has apparently increased in the Southern Hemisphere.

1. Introduction.

Determination of long-term (multi-decadal) variations in the Earth's mesosphere (60-100 km) is challenging. In situ measurements can only be made by rockets that provide a brief snapshot of local conditions. Ground-based measurements of key parameters (e.g. temperature, water vapor, winds) are only available at selected locations. While some data sets are quite long (e.g. phase height (Peters et al. (2017)), other potentially valuable data sets have gaps. Some relevant satellite datasets do exist (e.g. Upper Atmospheric Research Satellite (UARS) Halogen Occultation Experiment (HALOE) (Hervig and Siskind, 2006), Aura Microwave Limb Sounder (MLS) (Lambert et al., 2007; Schwarz et al., 2008), and Thermosphere-Ionosphere-Mesosphere Energetics and Dynamics (TIMED) Sounding of the Atmosphere using Broadband Radiometry (SABER) (Remsberg et al., 2008). However, since the lifetime of a single instrument is

© Author(s) 2018. CC BY 4.0 License.

generally limited to 10-15 years, maintaining continuity for a specific parameter over multiple decades again becomes an issue.

Another option is to measure an observable quantity that provides indirect information about the background state of the mesosphere. Polar mesospheric clouds (PMCs) are observed only at high latitudes (typically >50°) and high altitudes (80-85 km) during summer months in each hemisphere. They are formed from small ice crystals (~20-80 nm radius), whose formation and evolution are very sensitive to the temperature (< 150 K) and water vapor abundance near the mesopause. Recent work (e.g. Hervig et al. (2009), Rong et al. (2014), Hervig et al. (2015), Berger and Lübken (2015), Hervig et al. (2016)) has shown quantitative relationships between PMC observables (occurrence frequency, albedo, ice water content) and mesospheric temperature and water vapor.

The Solar Backscatter Ultraviolet (SBUV) instrument (Heath et al., 1975) was originally launched in 1978 to measure stratospheric profile and total column ozone, using nadir measurements of backscattered UV radiation between 250-340 nm at moderate spatial resolution (170 km x 170 km footprint). Thomas et al. (1991) showed that these measurements could also be analyzed to identify bright PMCs as an excess radiance signal above the Rayleigh-scattered sky background, modified by ozone absorption. These measurements have been extended by the second generation SBUV/2 instrument, which has been flown successfully on seven NOAA satellites from 1985 to the present. DeLand et al. (2003) describes the extension of the SBUV PMC detection algorithm to SBUV/2 measurements.

The consistent design of all SBUV/2 instruments allows the same PMC detection algorithm to be used with each data set, and the overlapping lifetime of these instruments (Figure 1) enables the creation of a merged data set long enough to be used for trend studies. Development and updates to this data set have been published by DeLand et al. (2006), DeLand et al. (2007), Shettle et al. (2009), and DeLand and Thomas (2015). Additional recent studies of long-term PMC behavior that use the SBUV PMC data set include Hervig and Stevens (2014), Berger and Lübken (2015), Hervig et al. (2016), Fiedler et al. (2017), Kuilman et al. (2017), and von Savigny et al. (2017).

© Author(s) 2018. CC BY 4.0 License.

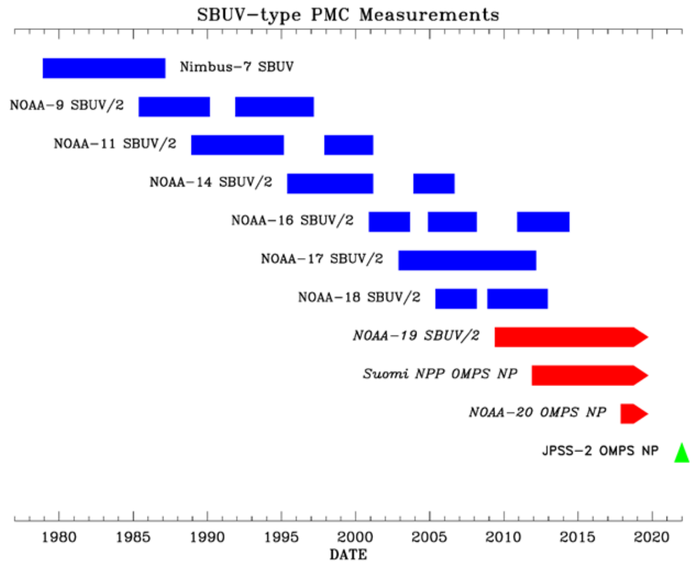

Figure 1. Timeline of SBUV instrument measurements used for PMC analysis. Blue color indicates inactive instruments. Arrowheads and red color indicate active instruments. Green color indicates planned instrument. Gaps for many SBUV/2 instruments reflect satellite drift into a near-terminator orbit where the current PMC detection algorithm does not function well.

The last SBUV/2 instrument is now flying on the NOAA-19 spacecraft. Its sun-synchronous orbit is drifting towards the terminator (current Equator-crossing time = 1615 LT), which will interrupt the ability to extract PMC information in 2019 or 2020 due to the decrease in solar zenith angle range available for daytime measurements. Fortunately, the SBUV measurement concept is being continued by the Ozone Mapping and Profiling Suite (OMPS) Nadir Profiler (NP) instrument (Seftor et al., 2014), which is now orbiting on two satellites. This paper will describe updated PMC trends that extend the work of DeLand and Thomas (2015), including the addition of OMPS NP data to the 40-year merged SBUV PMC dataset.

2. OMPS NP Data

© Author(s) 2018. CC BY 4.0 License.

The OMPS NP instrument was developed to provide ozone data that are consistent with the SBUV/2 series of instruments (Flynn et al., 2014). The first OMPS NP instrument was launched on the Suomi National Polar-orbiting Partnership (S-NPP) satellite on 28 October 2011, and began collecting regular data in January 2012. It makes hyperspectral measurements covering the 250-310 nm spectral region, with a sampling of approximately 0.6 nm. We utilize radiance measurements interpolated to the five shortest SBUV/2 wavelengths (nominally 252.0, 273.5, 283.1, 287.6, 292.3 nm) to provide continuity with the current SBUV PMC detection algorithm. Potential retrieval improvements based on a different wavelength selection will be explored in the future. The NP instrument uses a larger field of view (250 km x 250 km at the surface) compared to a SBUV/2 instrument. We will show that this difference does not affect the ability of the NP instrument to track seasonal PMC behavior.

The only revision implemented to the SBUV PMC detection algorithm for OMPS NP is to derive a solar zenith angle-dependent detection threshold in albedo that is based on NP end-of-season measurements. This update ensures that any change in background variability introduced by the larger NP field of view is addressed. Figure 2 shows the NP threshold function derived from data taken during August 2012. The SBUV/2 threshold function determined by DeLand and Thomas (2015) is shown for comparison, where an empirical scaling factor of 1.6 is also applied to eliminate "false positive" PMC detections at the start and end of the PMC season. These functions differ slightly at low solar zenith angle, but are almost identical at SZA > 50°. It is important to note that additional tests focusing on spectral dependence of the albedo residuals are also applied to positively identify any sample as a PMC.

© Author(s) 2018. CC BY 4.0 License.

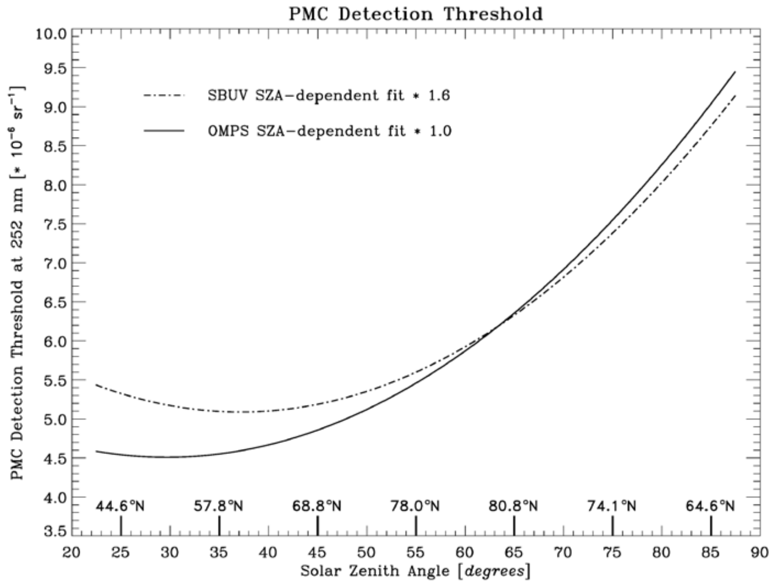

Figure 2. PMC detection threshold functions plotted *vs.* solar zenith angle (SZA). The quadratic fit in SZA used by DeLand and Thomas (2015) for SBUV/2 processing is shown as the dot-dash line, and the quadratic fit in SZA used for OMPS NP data in this paper is shown as the solid line. Nominal latitude values for June 21 are identified on the bottom of the plot.

We validate the S-NPP OMPS NP PMC data by comparing occurrence frequency and ice water content (IWC) seasonal average results to concurrent NOAA-19 SBUV/2 PMC results for 13 PMC seasons from Northern Hemisphere (NH) 2012 through NH 2018. IWC values are derived from PMC albedo values using the albedo-ice regression (AIR) approach described in DeLand and Thomas (2015). Figures 3-5 show these comparisons for the latitude bands 50°-64°, 64°-74°, and 74°-82° respectively. The two instruments agree very well in both absolute level and interannual variability for both quantities in each latitude band. The occurrence frequency difference between instruments in the NH 2016 season at 64°-74° N (Figure 4(a)) is anomalous, and does not appear in IWC results for the same season (Figure 4(b)). We are satisfied that S-NPP OMPS NP data can be added to the SBUV PMC data set to continue the long-term record in a consistent manner.

Atmos. Chem. Phys. Discuss., https://doi.org/10.5194/acp-2018-1034
Manuscript under review for journal Atmos. Chem. Phys.
Discussion started: 6 December 2018
© Author(s) 2018. CC BY 4.0 License.

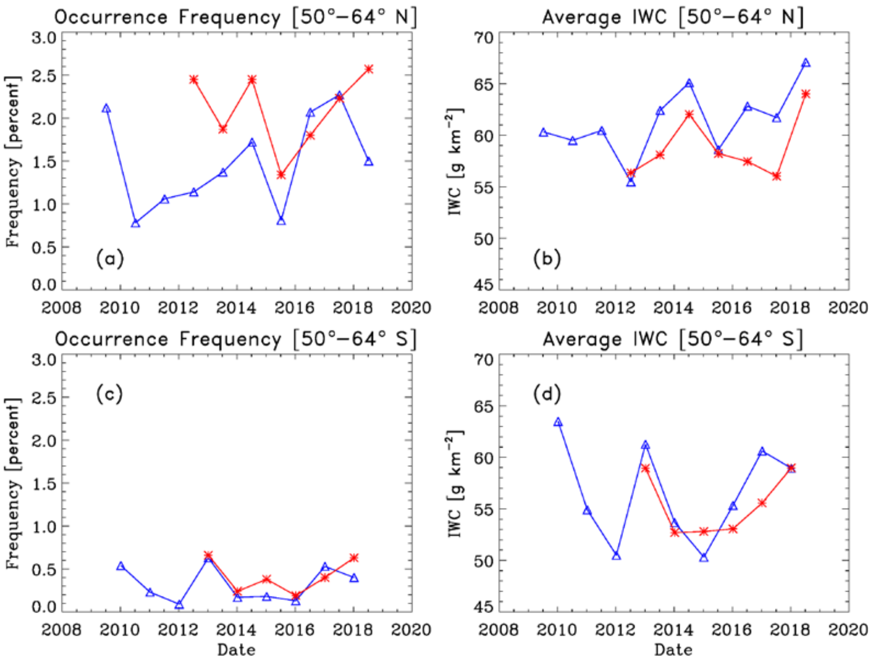

Figure 3. Season average PMC occurrence frequency and ice water content data at 50°-64° latitude. Blue = NOAA-19 SBUV/2, red = S-NPP OMPS. Left side = occurrence frequency [percent], right side = IWC [g km^{-2}]. Top row = Northern Hemisphere, bottom row = Southern Hemisphere.

© Author(s) 2018. CC BY 4.0 License.

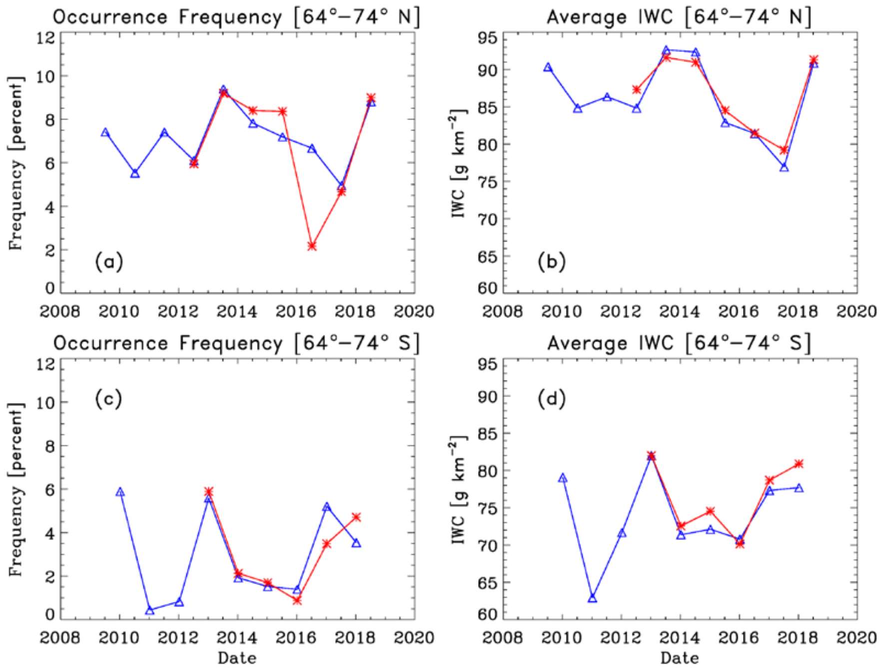

Figure 4. Season average occurrence frequency and IWC data at 64°-74° latitude. Identifications are as in Figure 3.

Atmos. Chem. Phys. Discuss., https://doi.org/10.5194/acp-2018-1034
Manuscript under review for journal Atmos. Chem. Phys.
Discussion started: 6 December 2018
© Author(s) 2018. CC BY 4.0 License.

Atmospheric Chemistry and Physics Discussions
Open Access
EGU

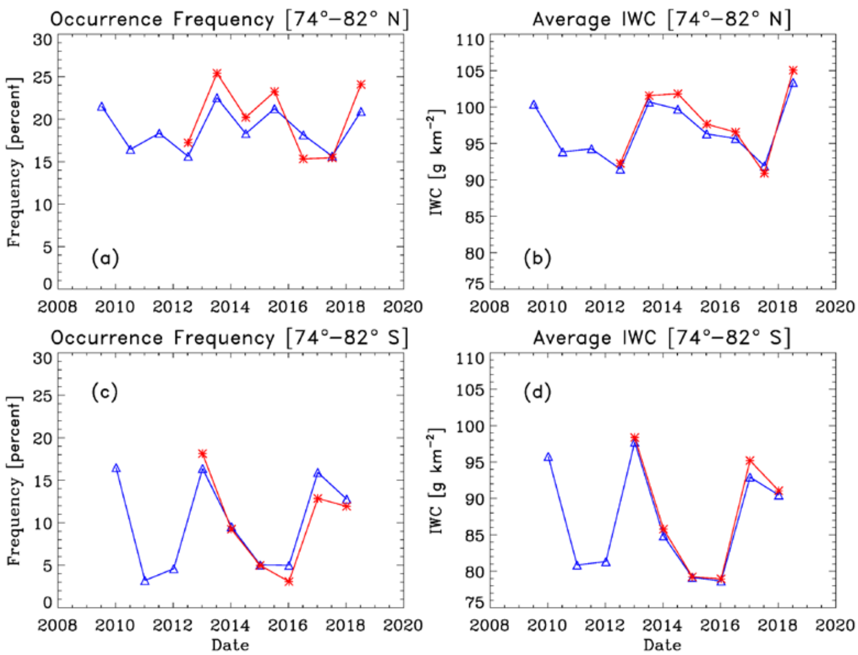

Figure 5. Season average occurrence frequency and IWC data at 74°-82° latitude. Identifications are as in Figure 3.

3. Trend Update

Our analysis of long-term trends in SBUV PMC data follows the approach presented in DeLand et al. (2007), and updated by DeLand and Thomas (2015). Briefly, we use a multiple regression fit of the form

$$X_{fit}(\text{latitude},t) = A(\text{latitude})*F_{Ly\alpha}(t) + B(\text{latitude})*(t-1979) + C(\text{latitude}) \qquad [1]$$

where $F_{Ly\alpha}(t)$ is the composite solar Lyman alpha flux dataset available from the LASP Interactive Solar Irradiance Data Center (LISIRD) and averaged over the appropriate NH or SH season. We define the duration of each season as [-20 days since solstice (DSS), +55 DSS] for SBUV trend analysis, following the discussion presented in DeLand and Thomas (2015).

© Author(s) 2018. CC BY 4.0 License.

We first created a merged SBUV PMC IWC data set for each season and latitude band, using an adaptation of the "backbone" method of Christy and Norris (2004) as discussed by DeLand et al. (2007). An advantage of this method is that it easily accommodates the addition of new instruments such as S-NPP OMPS NP to the overall PMC data set. Normalization adjustment values for each instrument derived from a fit at 50°-82° latitude are applied consistently at all latitude bands. The adjustment values for merging derived in this work are slightly different than those derived by DeLand and Thomas (2015) because the composition of the overall data set has changed, even though the original V4 PMC data sets for each instrument as described in that paper have not changed. Almost all adjustment values are still less than 3% of the seasonal average IWC (e.g. 0.97-1.03), and most of the changes determined for this paper relative to DeLand and Thomas (2015) are smaller than ±0.01.

Berger and Lübken (2011) suggested that the long-term trend in mesospheric temperature at 83 km changed from negative to positive in the late 1990s, based on 3-D atmospheric model runs driven by lower atmosphere reanalysis data. Since PMC properties are expected to be very responsive to mesospheric temperature changes, DeLand and Thomas (2015) followed this guidance and calculated their PMC trends in two segments, with a break point in 1998. We follow the same approach here and calculate multiple regression fits for two time segments, covering 1979-1997 and 1998-2018 respectively.

Atmos. Chem. Phys. Discuss., https://doi.org/10.5194/acp-2018-1034
Manuscript under review for journal Atmos. Chem. Phys.
Discussion started: 6 December 2018
© Author(s) 2018. CC BY 4.0 License.

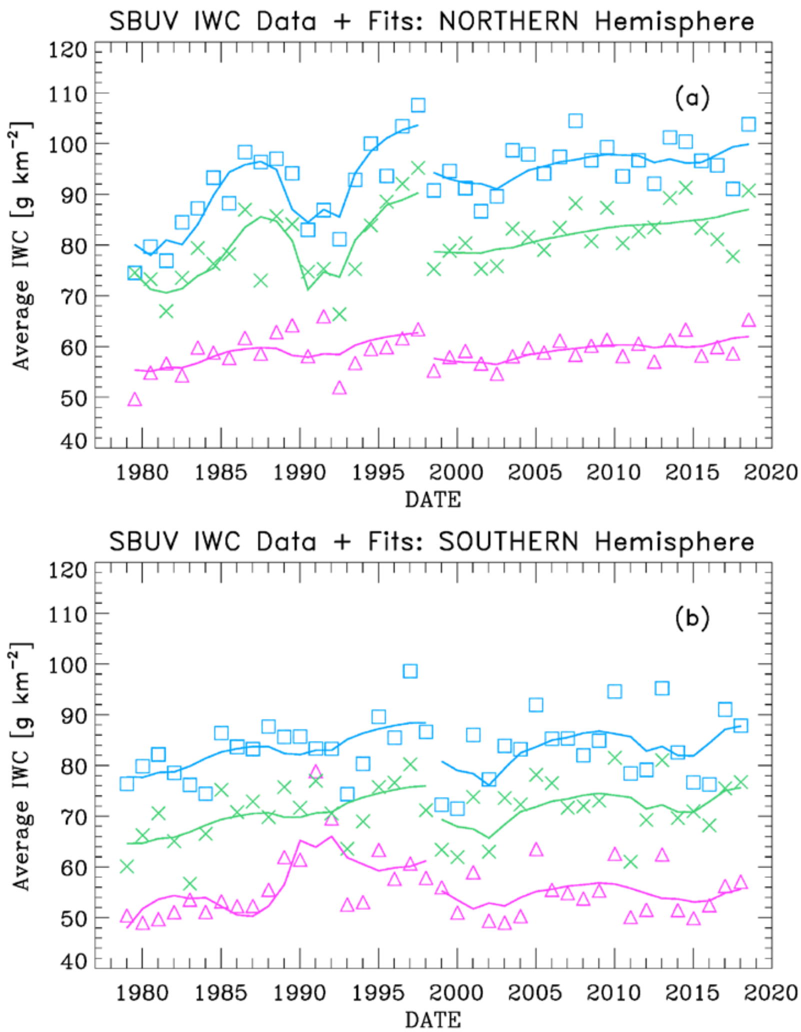

Figure 6. (a) SBUV merged seasonal average IWC values for three different latitude bands: 50°-64° N (purple triangles), 64°-74° N (green crosses), 74°-82° N (blue squares). The solid lines show multiple regression fits to the data for the periods 1979-1997 and 1998-2018. (b) SBUV merged seasonal average IWC values for 50°-64° S, 64°-74° S, and 74°-82° S. The solid lines show fits for the periods 1979-1997 and 1998-2018.

© Author(s) 2018. CC BY 4.0 License.

The results of these fits are shown in Figure 6, and presented numerically in Tables 1 and 2. Note that a negative sign for the solar activity term implies an anti-correlation, i.e. increase in solar activity corresponds to a decrease in IWC. This behavior has been explained by variations in solar ultraviolet irradiance, which causes higher temperatures and lower water vapor abundance during solar maximum periods (Garcia, 1989). We assess the significance of the trend term by calculating a 95% confidence limit as described in DeLand et al. (2007), using a method presented by Weatherhead et al. (1998) that accounts for auto-regression.

a. NH trends are significant for all latitude bands in both segments, although the trends for segment 2 are smaller than those derived in 2015.

b. SH trends are significant in segment 1, but not in segment 2. Note that the uncertainty in each SH latitude band fit is larger than the corresponding NH latitude band, indicating greater interannual variability in SH PMC data. This difference between hemispheres has been explained by Siskind et al. (2005) to be caused by higher SH mesospheric temperatures, making SH PMCs more sensitive to small temperature changes.

c. NH solar terms are large and significant in segment 1. Phase lag values of 0.5-1.0 years are found, consistent with previous analysis of SBUV PMC data. The solar term is smaller by a factor of three to six and marginally significant for segment 2, depending on latitude band. This lack of response to solar activity in recent years has also been identified in ALOMAR lidar PMC data (Fiedler et al., 2017) and AIM CIPS data (Siskind et al., 2013).

d. The calculated SH solar term is small and not significant in segment 1, but above 64° latitude is two to three times larger for segment 2 and becomes statistically significant. The large positive solar term at 50°-64° S is driven by higher IWC values in the 1990-1991 and 1991-1992 seasons. However, in this latitude band, only 10-20 clouds are detected during the entire seasons in some years. Fluctuations in only a few samples can thus have a significant impact in such seasons.

We speculate that during segment 2, the multiple regression fit algorithm is assigning some of the greater interannual variability in SH data to the solar activity term. This result illustrates the need for caution in interpreting the results of using a periodic term based on solar variability in a regression fit that covers less than two full solar cycles, since variations in a small number of data points near the end of the period can have a substantial impact. However, the large IWC

Atmos. Chem. Phys. Discuss., https://doi.org/10.5194/acp-2018-1034
Manuscript under review for journal Atmos. Chem. Phys.
Discussion started: 6 December 2018
© Author(s) 2018. CC BY 4.0 License.

values observed in the recent NH 2018 PMC season did not significantly change the NH solar activity term for this segment. The source of the hemispheric difference in solar activity response is not yet understood.

4. Conclusion

We have shown that OMPS NP measurements can be used successfully to continue the long PMC data record created from SBUV and SBUV/2 instruments. When we use S-NPP data to extend our merged PMC data set through the NH 2018 season, we find smaller trends in IWC in both hemispheres since 1998 compared to the results shown by DeLand and Thomas (2015). The NH trends continue to be significant at the 95% confidence level, while the SH trends are now slightly smaller than this threshold. The calculated sensitivity to solar activity during 1998-2018 is a factor of three to six smaller than the 1979-1997 result for NH data above 64° N. However, the solar activity sensitivity for SH data increases by a factor of three to four for the 1998-2018 period, and becomes statistically significant at all latitudes. We will continue to investigate possible causes for this change in behavior and hemispheric discrepancy.

A second OMPS NP instrument was launched on the NOAA-20 (formerly JPSS-1) satellite in November 2017, and is now collecting regular data. Three more OMPS NP instruments are scheduled for launch on JPSS satellites at regular intervals through approximately 2030. All of the satellites carrying OMPS NP instruments will be kept in an afternoon equator-crossing time sun-synchronous orbit, so that orbit drift (which has impacted all SBUV/2 instruments) will not affect the ability to retrieve PMC information. We therefore anticipate extending the continuous SBUV PMC data record to 60 years to support long-term climate studies.

Data Availability. Daily IWC data for all SBUV instruments during every season are available on-line at https://sbuv2.gsfc.nasa.gov/pmc/v4/. A text file describing the contents of these files is also provided. Solar Lyman alpha flux data is available at http://lasp.colorado.edu/lisird/.

© Author(s) 2018. CC BY 4.0 License.

Author Contributions. MD processed the SBUV and OMPS PMC data, conducted the regression fit analysis, and wrote the primary manuscript. GT reviewed and edited the manuscript.

Acknowledgements. We greatly appreciate the continuing efforts of Larry Flynn and many other people at NOAA STAR to provide high quality SBUV/2 and OMPS NP data that enable the creation of our PMC product. M. T. DeLand was supported by NASA grant NNH12CF94C. G. Thomas was supported by the NASA AIM mission, which is funded by NASA's Small Explorers Program under contract NAS5-03132.

© Author(s) 2018. CC BY 4.0 License.

References

Berger, U., and Lübken, F.-J.: Mesospheric temperature trends at mid-latitudes in summer, Geophys. Res. Lett., 38, L22804, doi:10.1029/2011GL049528, 2011.

Berger, U., and Lübken, F.-J.: Trends in mesospheric ice layers in the Northern Hemisphere during 1961-2013, J. Geophys. Res. Atmos., 120, doi:10.1002/2015JD023355, 2015.

Christy, J. R., and Norris, W. B.: What may we conclude about global temperature trends?, Geophys. Res. Lett., 31, L06211, doi:10.1029/2003GL019361, 2004.

DeLand, M. T., and Thomas, G. E.: Updated PMC trends derived from SBUV data, J. Geophys. Res. Atmos., 120, doi:10.1002/2014JD022253, 2015.

DeLand, M. T., Shettle, E. P., Thomas, G. E., and Olivero, J. J.: Solar backscattered ultraviolet (SBUV) observations of polar mesospheric clouds (PMCs) over two solar cycles, J. Geophys. Res., 108(D8), 8445, doi:10.1029/2002JD002398, 2003.

DeLand, M. T., Shettle, E. P., Thomas, G. E., and Olivero, J. J.: A quarter-century of satellite PMC observations, J. Atmos. Solar-Terr. Phys., 68, 9-29, 2006.

DeLand, M. T., Shettle, E. P., Thomas, G. E., and Olivero, J. J.: Latitude-dependent long-term variations in polar mesospheric clouds from SBUV Version 3 PMC data, J. Geophys. Res., 112, D10315, doi:10.1029/2006JD007857, 2007.

Fiedler, J., Baumgarten, G., Berger, U., and Lübken, F.-J.: Long-term variations of noctilucent clouds at ALOMAR, J. Atmos. Solar-Terr. Phys., 162, 79-89, doi:10.1016/j.jastp.2016.08.006, 2017.

Flynn, L., Long, C., Wu, X., Evans, R., Beck, C. T., Petropavlovskikh, I., McConville, G., Yu, W., Zhang, Z., Niu, J., Beach, E., Hao, Y., Pan, C., Sen, B., Novicki, M., Zhou, S., and Seftor, C.: Performance of the Ozone Mapping and Profiling Suite products, J. Geophys. Res. Atmos., 119, 6181-6195, doi:10.1002/2013JD020467, 2014.

Garcia, R. R.: Dynamics, radiation, and photochemistry in the mesosphere: Implications for the formation of noctilucent clouds, J. Geophys. Res., 94, 14605-14615, 1989.

Heath, D. F., Krueger, A. J., Roeder, H. A., and Henderson, B. D.: The Solar Backscatter Ultraviolet and Total Ozone Mapping Spectrometer (SBUV/TOMS) for Nimbus G, Opt. Eng., 14, 323-331, 1975.

Hervig, M., and Siskind, D.: Decadal and inter-hemispheric variability in polar mesospheric clouds, water vapor, and temperature, J. Atmos. Solar Terr. Phys., 68, 30-41, doi:10.1016/j.jastp.2005.08.010, 2006

© Author(s) 2018. CC BY 4.0 License.

Hervig, M. E., and Stevens, M. H.: Interpreting the 35-year SBUV PMC record with SOFIE observations, J. Geophys. Res. Atmos., 119, doi:10.1002/2014JD021923, 2014.

Hervig, M. E., Stevens, M. H., Gordley, L. L., Deaver, L. E., Russell III, J. M., and Bailey, S. M.: Relationships between polar mesospheric clouds, temperature, and water vapor from Solar Occultation for Ice Experiment (SOFIE) observations, J. Geophys. Res., 114, D20203, doi:10.1029/2009JD012302, 2009.

Hervig, M. E., Siskind, D. E., Bailey, S. M., and Russell III, J. M.: The influence of PMCs on water vapor and drivers behind PMC variability from SOFIE observations, J. Atmos. Solar Terr. Phys., 132, 124-134, doi:10.1016/j.jastp.2015.07.010, 2015.

Hervig, M. E., Berger, U., and Siskind, D. E.: Decadal variability in PMCs and implications for changing temperature and water vapor in the upper mesosphere, J. Geophys. Res. Atmos., 121, 2383-2392, doi:10.1002/2015JD024439, 2016.

Kuilman, M., Karlsson, B., Benze, S., and Megner, L.: Exploring noctilucent cloud variability using the nudged and extended version of the Canadian Middle Atmosphere Model, J. Atmos. Solar-Terr. Phys., 164, 276-288, doi:10.1016/j.jastp.2017.08.019, 2017.

Lambert, A., Read, W. G., Livesey, N. J., Santee, M. L., Manney, G. L., Froidevaux, L., Wu, D. L., Schwartz, M. J., Pumphrey, H. C., Jimenez, C., Nedoluha, G. E., Cofield, R. E., Cuddy, D. T., Daffer, W. H., Drouin, B. J., Fuller, R. A., Jamot, R. F., Knosp, B. W., Pickett, H. M., Perun, V. S., Snyder, W. V., Stek, P. C., Thurstans, R. P., Wagner, P. A., Waters, J. W., Jucks, K. W., Toon, G. C., Stachnik, R. A., Bernath, P. A., Boone, C. D., Walker, K. A., Urban, J., Murtagh, D., Elkins, J. W., and Atlas, E.: Validation of the Aura Microwave Limb Sounder middle atmosphere water vapor and nitrous oxide measurements, J. Geophys. Res., 112, D24S36, doi:10.1029/2007JD008724, 2007.

Peters, D. H. W., Entzian, G., and Keckhut, P.: Mesospheric temperature trends derived from standard phase-height measurements, J. Atmos. Solar Terr. Phys., 163, 23-30, doi:10.1016/j.jastp.2017.04.007, 2017.

Remsberg, E. E., Marshall, B. T., Garcia-Comas, M., Krueger, D., Lingenfelser, D. L., Martin-Torres, J., Mlynczak, M. G., Russell III, J. M., Smith, A. K., Zhao, Y., Brown, C., Gordley, L. L., Lopez-Gonzales, M. J., Lopez-Puertas, M., She, C.-Y., Taylor, M. J., and Thompson, R. E.: Assessment of the quality of the Version 1.07 temperature-versus-pressure profiles of the middle atmosphere from TIMED/SABER, J. Geophys. Res., 113, D17101, doi:10.1029/2008JD010013, 2008.

Rong, P. P., Russell III, J. M., Randall, C. E., Bailey, S. M., and Lambert, A.: Northern PMC brightness zonal variability and its correlation with temperature and water vapor, J. Geophys. Res. Atmos., 119, 2390-2408, doi:10.1002/2013JD020513, 2014.

Schwartz, M. J., Lambert, A., Manney, G. L., Read, W. G., Livesey, N. J., Froidevaux, L., Ao, C. O., Bernath, P. A., Boone, C. D., Cofield, R. E., Daffer, W. H., Drouin, B. J., Fetzer,

© Author(s) 2018. CC BY 4.0 License.

E. J., Fuller, R. A., Jamot, R. F., Jiang, J. H., Jiang, Y. B., Knosp, B. W., Krüger, K., Li, J.-L. F., Mlynczak, M. G., Pawson, S., Russell III, J. M., Santee, M. L., Snyder, W. V., Stek, P. C., Thurstans, R. P., Tompkins, A. M., Wagner, P. A., Walker, K. A., Waters, J. W., and Wu, D. L.: Validation of the Aura Microwave Limb Sounder temperature and geopotential height measurements, J. Geophys. Res., 113, D15S11, doi:10.1029/2007JD008783, 2008.

Seftor, C. J., Jaross, G., Kowitt, M., Haken, M., Li, J., and Flynn, L. E.: Postlaunch performance of the Suomi National Polar-orbiting Partnership Ozone Mapping and Profiler Suite (OMPS) nadir sensors, J. Geophys. Res. Atmos., 119, doi:10.1002/2013JD020472, 2014.

Shettle, E. P., DeLand, M. T., Thomas, G. E., and Olivero, J. J.: Long term variations in the frequency of polar mesospheric clouds in the Northern Hemisphere from SBUV, Geophys. Res. Lett., 36, L02803, doi:10.1029/2008GL036048, 2009.

Siskind, D. E., Stevens, M. H., and Englert, C. E.: A model study of global variability in mesospheric cloudiness, J. Atmos. Solar Terr. Phys., 67, 501-513, doi:10.1016/j.jastp.2004.11.007, 2005.

Siskind, D. E., Stevens, M. H., Hervig, M. E., and Randall, C. E.: Recent observations of high mass density polar mesospheric clouds: A link to space traffic?, Geophys. Res. Lett., 40, 2813-2817, doi:10.1002/grl.50540, 2013.

Thomas, G. E., McPeters, R. D., and Jensen, E. J.: Satellite observations of polar mesospheric clouds by the Solar Backscattered Ultraviolet radiometer: Evidence of a solar cycle dependence, J. Geophys. Res., 96, 927-939, 1991.

von Savigny, C., DeLand, M. T., and Schwartz, M. J.: First identification of lunar tides in satellite observations of noctilucent clouds, J. Atmos. Solar-Terr. Phys., 162, 116-121, doi:10.1016/j.jastp.2016.07.002, 2017.

Weatherhead, E. C., Reinsel, G. C., Tiao, G. C., Meng, X.-L., Choi, D., Cheang, W.-K., Keller, T., DeLuisi, J., Wuebbles, D. J., Kerr, J. B., Miller, A. J., Oltmans, S. J., and Frederick, J. E.: Factors affecting the detection of trends: Statistical considerations and applications to environmental data, J. Geophys. Res., 103, 17,149-17,161, 1998.

© Author(s) 2018. CC BY 4.0 License.

Table 1(a)

Regression Fit Results for IWC, Northern Hemisphere, 1979-1997

Latitude	A(±dA)	R_{time}	B(±dB)	R_{solar}	C	Lag	Trend	Conf	Cycle
50-64 N	0.28(±0.14)	0.50	-1.27(±0.87)	-0.44	62.1	0.5	**4.8**	2.3	-5.5
64-74 N	0.47(±0.22)	0.57	-6.41(±1.53)	-0.77	104.6	1.0	**6.0**	3.3	-20.5
74-82 N	0.65(±0.22)	0.70	-6.52(±1.38)	-0.82	115.2	0.5	**7.2**	2.8	-18.3
50-82 N	0.62(±0.21)	0.70	-5.89(±1.32)	-0.81	108.3	0.5	**7.1**	2.7	-17.3

Table 1(b)

Regression Fit Results for IWC, Northern Hemisphere, 1998-2018

Latitude	A(±dA)	R_{time}	B(±dB)	R_{solar}	C	Lag	Trend	Conf	Cycle
50-64 N	0.20(±0.11)	0.59	-1.05(±1.09)	-0.45	57.9	0.5	**3.4**	0.9	-4.5
64-74 N	0.42(±0.18)	0.57	-0.82(±2.02)	-0.27	73.5	1.0	**5.1**	1.6	-2.5
74-82 N	0.24(±0.18)	0.44	-2.21(±1.75)	-0.43	98.1	0.5	**2.6**	1.5	-5.8
50-82 N	0.30(±0.17)	0.49	-1.48(±1.66)	-0.36	88.8	0.5	**3.3**	1.5	-4.1

Table 2(a)

Regression Fit Results for IWC, Southern Hemisphere, 1979-1997

Latitude	A(±dA)	R_{time}	B(±dB)	R_{solar}	C	Lag	Trend	Conf	Cycle
50-64 S	0.98(±0.26)	0.54	+4.87(±1.92)	+0.19	24.9	0.5	**17.3**	5.1	+21.8
64-74 S	0.51(±0.23)	0.59	-1.06(±1.54)	-0.41	70.3	0.0	**7.3**	4.6	-3.8
74-82 S	0.45(±0.25)	0.57	-1.38(±1.65)	-0.44	85.3	0.0	**5.4**	4.5	-4.2
50-82 S	0.53(±0.24)	0.61	-0.94(±1.60)	-0.41	79.9	0.0	**6.6**	4.4	-3.0

Table 2(b)

Regression Fit Results for IWC, Southern Hemisphere, 1998-2018

Atmos. Chem. Phys. Discuss., https://doi.org/10.5194/acp-2018-1034
Manuscript under review for journal Atmos. Chem. Phys.
Discussion started: 6 December 2018
© Author(s) 2018. CC BY 4.0 License.

Latitude	A(±dA)	R_{time}	B(±dB)	R_{solar}	C	Lag	Trend	Conf	Cycle
50-64 S	-0.08(±0.27)	0.07	-2.97(±2.83)	-0.32	69.7	0.5	-1.4	2.5	-13.8
64-74 S	0.15(±0.23)	0.32	-3.38(±2.05)	-0.44	81.9	0.0	2.1	2.4	-12.0
74-82 S	0.14(±0.24)	0.31	-4.22(±2.18)	-0.46	97.4	0.0	1.7	2.6	-12.9
50-82 S	0.14(±0.23)	0.31	-3.92(±2.12)	-0.46	92.2	0.0	1.7	2.6	-12.2

Multiple regression fit parameters for SBUV merged seasonal average IWC data, using the form

$$IWC = A*(t_{center} - 1979.0) + B*F_{Ly\alpha}(t_{center} - t_{lag}) + C$$

t_{center} = mid-point of PMC season (DSS = [-20,+55]) [years]

$F_{Ly\alpha}$ = Lyman alpha flux averaged over PMC season, scaled by $1x10^{11}$ photons cm^{-2} sec^{-1} nm^{-1}

R_{time} = correlation coefficient of secular term

R_{solar} = correlation coefficient of solar term

t_{lag} = phase lag of solar term for fit with smallest χ^2 value [years]

Trend = decadal change in IWC [%]. **Bold** values exceed 95% confidence level.

Conf = amount of decadal change required to exceed 95% confidence level [%]

Cycle = calculated variation in IWC from solar minimum to solar maximum [%], using a Lyman alpha flux range of $2.6x10^{11}$ photons cm^{-2} sec^{-1} nm^{-1}